


Enhanced acousto-optic properties of Silicon carbide based layered structure

Namrata Dewan Soni

Department of Physics, Hansraj College, University of Delhi, Delhi, India

Follow this and additional works at: <https://bjeps.alkafeel.edu.iq/journal>

 Part of the [Condensed Matter Physics Commons](#), and the [Optics Commons](#)

Recommended Citation

Soni, Namrata Dewan (2023) "Enhanced acousto-optic properties of Silicon carbide based layered structure," *Al-Bahir*. Vol. 3: Iss. 1, Article 6.

Available at: <https://doi.org/10.55810/2313-0083.1035>

This Original Study is brought to you for free and open access by Al-Bahir. It has been accepted for inclusion in Al-Bahir by an authorized editor of Al-Bahir. For more information, please contact bjeps@alkafeel.edu.iq.

ORIGINAL STUDY

Enhanced Acousto-Optic Properties of Silicon Carbide-Based Layered Structure

Namrata D. Soni

Department of Physics, Hansraj College, University of Delhi, Delhi, India

Abstract

This study investigates the feasibility of using silicon carbide-based layered surface acoustic wave (SAW) devices in acousto-optic applications. The acousto-optic properties of the temperature-stable layered structure $\text{TeO}_2/\text{SiC}/128^\circ\text{Y-X LiNbO}_3$ are investigated through theoretical analysis. This analysis includes the evaluation of key parameters such as the overlap integral, figure of merit, and diffraction efficiency. The SAW propagation characteristics and field profiles required for these calculations are obtained using SAW software. Results show that the layered structure has high diffraction efficiency of nearly 96% and a promising value for the acousto-optic figure of merit, indicating potential use in low driving power acousto-optic devices. The study concludes that the 3C-SiC-based layered structure possesses excellent acousto-optic properties and has potential for use in acousto-optic devices that can withstand harsh environmental conditions.

Keywords: Acousto-optic effects, Lithium niobate, Silicon carbide, Thermal stability

1. Introduction

The domain of photonics encompasses a variety of acousto-optic devices such as tunable optical filters, modulators, Q-switches, optical deflectors, etc. [1–5], which find applications in diverse fields like optical metrology, neuroscience, high content screening, military, agronomy, entertainment, etc. [6–10]. The basic principle underlying the functioning of an acousto-optic device is the diffraction of an optical wave by a high-frequency acoustic wave traveling on a piezoelectric crystal. The efficacy of an acousto-optic device depends upon the properties of the material medium on which the acoustic wave propagates [11,12]. So far, acoustic devices based on Lithium Niobate (LiNbO_3), Lithium tantalate (LiTaO_3) single crystals, and various layered structures like $\text{ZnO}/\text{SiO}_2/\text{Si}$, $\text{TeO}_{2+x}/\text{LiNbO}_3$, $\text{BeO}/\text{LiNbO}_3$, $\text{LiNbO}_3/\text{Sapphire}$, $\text{ZnO}/\text{Diamond}$, etc., have been investigated [11,13–17]. With the advent of technology, multi-layered acoustic devices are preferred over the single crystal-based acoustic devices, as in the former, various properties like acoustic velocity;

electromechanical coupling coefficient and temperature coefficient of delay (TCD) can be easily tuned according to the application's needs [18–20].

The field of acousto-optics has witnessed significant advancements in recent years, primarily driven by the development of novel film preparation techniques and the utilization of advanced materials such as silicon carbide (SiC), zinc oxide (ZnO), zinc sulfide (ZnS), and perovskite-based materials [21–26]. These advancements have revolutionized the design and performance of acousto-optic wave devices, offering numerous advantages over conventional techniques and alternative systems. One of the key advantages of the film preparation techniques employed in the fabrication of acousto-optic wave devices is their superior control over the film's thickness, composition, and morphology [22]. These techniques, which include methods like pulsed laser deposition, chemical vapor deposition, and sol-gel synthesis, enable precise engineering of the film properties at the nano-scale. This level of control allows for the optimization of the acousto-optic interaction, resulting in enhanced device performance and improved efficiency [22].

Received 8 May 2023; revised 28 May 2023; accepted 29 May 2023.

Available online 14 July 2023

E-mail address: ndsoni@hrc.du.ac.in.

<https://doi.org/10.55810/2313-0083.1035>

2313-0083/© 2023 University of AlKafeel. This is an open access article under the CC-BY-NC license (<http://creativecommons.org/licenses/by-nc/4.0/>)

Recent reports uncover the potential of silicon carbide for usage in a multi-layered acoustic device [26–29]. In 2018, Soni reported a temperature-stable TeO_3 (0.007 λ)/3C–SiC (0.09 λ)/128°Y–X LiNbO₃ multi-layered SAW configuration based on the sturdy crystalline 3C–SiC material and found it suitable for high-frequency applications as it possesses high values of acoustic velocity ($\sim 4390 \text{ ms}^{-1}$) and electromechanical coupling coefficient ($\sim 9.8\%$) [27,30]. The layered structure is reported to become temperature-stable at a normalized TeO_3 over-layer thickness of 0.007 λ . There exist reports that demonstrate the significant use of SiC in the field of photonics and optoelectronics [31–33]. It has been well established that relative to materials like zinc oxide (ZnO), zinc sulphide (ZnS), and perovskite-based materials, silicon carbide (SiC) has an edge for acousto-optic wave devices due to its physical properties; wide band-gap as this versatility expands the potential applications of SiC-based acousto-optic devices across a broad range of wavelengths; material availability and cost-effectiveness; high acousto-optic interaction efficiency [34]. The main focus of this research is to investigate and analyses the acousto-optic characteristics of thermally stable TeO_3 (0.007 λ)/3C–SiC (0.09 λ)/128°Y–X LiNbO₃ multi-layered configuration. The objective is to understand how this configuration performs in terms of its acousto-optic properties.

Hence, in the present study, the acousto-optic properties (figure of merit, diffraction efficiency) of the thermally stable TeO_3 (0.007 λ)/3C–SiC (0.09 λ)/128°Y–X LiNbO₃ layered acoustic device are explored using theoretical calculations. The thermally stable multi-layered configuration TeO_3 /3C–SiC/128°Y–X LiNbO₃ is found to be very promising, as it presents a high value of acousto-optic figure of merit $M = 8.56 \times 10^{-12} \text{ s}^3 \text{ kg}^{-1}$ and high diffraction efficiency.

2. Theoretical calculations

The present study theoretically investigates the acousto-optic properties, i.e., figure of merit and diffraction efficiency of a temperature-stable multi-layered TeO_3 (0.007 λ)/3C–SiC (0.09 λ)/128°Y–X LiNbO₃ configuration (shown in Fig. 1(a)).

Fig. 1. (b) shows the coordinate system considered in the present study to estimate the acoustic properties. Here, X_1 is the direction of propagation of the surface wave whose amplitude vanishes as X_3 tends to the negative of infinity. The requisite field profile and acoustic wave propagation characteristics of the TeO_3 (0.007 λ)/3C–SiC (0.09 λ)/128°Y–X LiNbO₃ layered structure have been determined

using the surface acoustic wave simulation software [35].

The material parameters, such as elastic constants, density, refractive index, dielectric constant, and photo-elastic constants, used in the present study, have been listed in Table 1.

2.1. Acousto-optic figure of merit

The efficacy of an acousto-optic device is essentially determined by its figure of merit. The figure of merit for the layered structure is defined as follows [17]:

$$M = \frac{n^6 P^2}{\rho v_p^3} \quad (1)$$

Here, P and n are the respective appropriate photo-elastic tensor and refractive index of the wave-guiding layer.

2.2. Overlap integral

To gauge the interaction between the acoustic and optical fields, the parameter employed is the overlap integral $|\Gamma_{mn}(f)|$. The expression for $|\Gamma_{mn}(f)|$ is given by [42]:

$$|\Gamma_{mn}(f)|^2 = \frac{\left[\int U_m(x_3) U_n(x_3) U_{ap} dx_3 \right]^2}{\int |U_m|^2(x_3) dx_3 \int |U_n|^2(x_3) dx_3} \quad (2)$$

Here, $U_{ap} = [p : S_a(x_3) + r : E_p U_p(x_3)]$.

where U_m and U_n represent the field distributions of the diffracted and un-diffracted modes, respectively. ' p ' and ' r ' are appropriate photo-elastic and electro-optic tensors, respectively.

2.3. Diffraction efficiency

Another significant factor in estimating the effectiveness of an acousto-optic device is its ability to diffract the optical signal, i.e., diffraction efficiency, which can be calculated as follows [42]:

$$DE = DE(f)_o^2 \left[\frac{\sin \sqrt{DE(f)_o^2 + \left(\frac{K \Delta \omega L}{2}\right)^2}}{\sqrt{DE(f)_o^2 + \left(\frac{K \Delta \omega L}{2}\right)^2}} \right]^2 \quad (3)$$

where L is the interaction length or acoustic aperture, λ is the free space optical wavelength, K is the

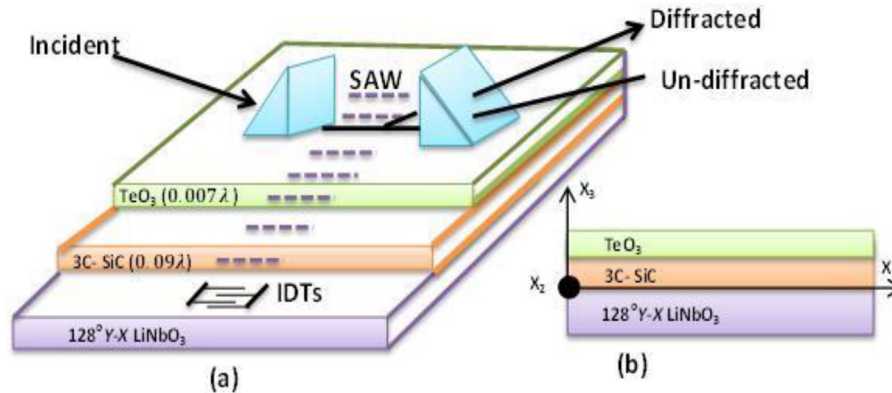


Fig. 1. (a): Configuration of layered Acousto-optic device proposed in present work. (b): The coordinate system used in the present work.

momentum vector of SAW, and $\Delta\Theta$ is the variation of the incident wave from the Bragg angle.

$$DE(f)_o^2 = \left(\frac{\pi}{\lambda_o}\right)^2 n_m n_n^2 |\Gamma_{mn}(f)|^2 \left(\frac{L}{\cos \Theta_m \cos \Theta_n}\right) \quad (4)$$

Table 1. Material parameters used in present study.

Material	TeO ₃ (Tellurium trioxide) [14,40]	SiC (Silicon Carbide) [36,38,39]	LiNbO ₃ (Lithium Niobate) [37,41]
Elastic Constants (10¹¹ Nm⁻²)			
C ₁₁	0.14	3.95	1.98
C ₃₃			2.279
C ₆₆			0.728
C ₄₄	0.265	2.36	0.5965
C ₁₂		1.23	0.5472
C ₁₃			0.6513
C ₁₄			0.0788
Piezoelectric constant (Cm⁻²)			
e ₃₃			1.77
e ₃₁			0.30
e ₁₅			3.69
e ₂₂			2.42
e ₁₄		-0.349	
Dielectric constant (10⁻¹¹ Fm⁻¹)			
ε ₁₁	23.7	7.01	45.6
ε ₃₃			26.3
Density (Kg m⁻³)			
ρ	4578	3210	4628
Photo-elastic constants			
P ₁₁	0.0074	-0.108	-0.021
P ₁₂	0.187	-0.0276	0.060
P ₁₃	0.34		0.172
P ₃₁	0.0905		0.141
P ₃₃	0.24		0.118
P ₄₄	-0.17	-0.087	0.121
P ₆₆	-0.043		
P ₁₄			-0.052
P ₄₁			-0.109
Refractive index			
n	2.2	2.5	2.3

The acousto-optic diffraction efficiency varies directly with the overlap $|\Gamma_{mn}(f)|$ between the acoustic and optical fields.

Equations (2), (3) and (4) are solved using a program written in the C language to calculate the overlap integral and hence the diffraction efficiency.

3. Result and Discussion

3.1. Figure of merit

The temperature-stable TeO₃ (0.007λ)/3C-SiC (0.09λ)/128°Y-X LiNbO₃ multi-layered configuration exhibits a high value of the figure of merit, i.e., $M = 8.56 \times 10^{-12} \text{ s}^3 \text{ kg}^{-1}$.

The value of the acousto-optic figure of merit obtained in this study is compared with that of some well-known materials or layered structures used in acousto-optic devices. The comparison is presented in Table 2.

The temperature-stable multi-layered configuration TeO₃/3C-SiC/128°Y-X LiNbO₃ exhibits remarkable acousto-optic properties, as highlighted in Table 2. In fact, it boasts the highest reported acousto-optic figure of merit among the various materials or layered structures examined. The figure of merit for this configuration is nearly seven times higher than that of the commonly used acousto-optic crystal, Tellurium dioxide ($M = 1143.8 \times 10^{-15} \text{ s}^3 \text{ kg}^{-1}$) [45].

Table 2. AO Figure of merit of various acousto-optic materials or multi-layered structures reported earlier and in present study.

Acousto-optic material/ layered structure	AO Figure of Merit ($\times 10^{-15} \text{ s}^3 \text{ Kg}^{-1}$)	Reference
LiNbO ₃	12.9	[43]
TeO ₂	1143.8	[44]
ZnO/AlN/Sapphire	3000.0	[42]
TeO ₃ /3C-SiC/128°Y-X LiNbO ₃	8560.0	(Present work)

This exceptional value of the acousto-optic figure of merit signifies the potential of the $\text{TeO}_3/3\text{C-SiC}/128^\circ\text{Y-X LiNbO}_3$ configuration in the development of high-performance acousto-optic devices. The high figure of merit indicates that this configuration can effectively modulate light with minimal power requirements, making it highly desirable for energy-efficient acousto-optic applications.

These findings underscore the significance of the proposed $\text{TeO}_3/3\text{C-SiC}/128^\circ\text{Y-X LiNbO}_3$ multi-layered configuration in the field of acousto-optics. Its superior acousto-optic figure of merit positions it as a promising candidate for the design and implementation of advanced acousto-optic devices that demand low driving power. This configuration holds considerable potential for a range of acousto-optic applications, further emphasizing its technological importance and the possibilities it brings to the field.

3.2. Overlap integral

The overlap integral of the $\text{TeO}_3/3\text{C-SiC}/128^\circ\text{Y-X LiNbO}_3$ multi-layered configuration is calculated using Equation (2) by varying the acoustic depth from 0 to 0.1λ . Fig. 2 shows the variation of the overlap integral factor with the normalized acoustic depth. Our results indicate that the greatest overlap between the acoustic and optical fields occurs in the absence of temperature-compensated TeO_3 over-layer. With the integration of TeO_3 layer, the overlap integral factor slightly decreases, which may be due to the integration of the over-layer stiffening the surface and raising the stress, altering the potential at the interface [46]. The

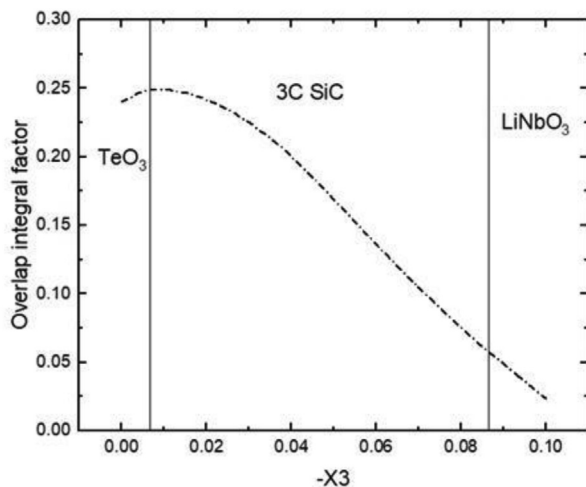


Fig. 2. Overlap integral factor as a function of normalized acoustic depth ($-X_3$) in $\text{TeO}_3 (0.007\lambda)/3\text{C-SiC} (0.09\lambda)/128^\circ\text{Y-X LiNbO}_3$ multi-layered configuration.

higher value of overlap integral near the surface suggests higher diffraction efficiency at lower penetration depth.

3.3. Diffraction efficiency

The diffraction efficiency of the $\text{TeO}_3 (0.007\lambda)/3\text{C-SiC} (0.09\lambda)/128^\circ\text{Y-X LiNbO}_3$ multi-layered configuration is calculated as a function of normalized penetration depth ($-X_3$) using equation (3). The results show that the maximum value of diffraction efficiency (approximately 96.1%) is obtained at the top of the silicon carbide layer, and it decreases slightly (within 4%) with the addition of the temperature-compensated TeO_3 over-layer. This reduction in diffraction efficiency is insignificant and can be overlooked for a "thermally stable" $\text{TeO}_3 (0.007\lambda)/3\text{C-SiC} (0.09\lambda)/128^\circ\text{Y-X LiNbO}_3$ multi-layered acoustic device. Therefore, the results suggest that this multi-layered configuration is an effective device for acousto-optic applications, with a diffraction efficiency of approximately 96.1%.

4. Conclusion

In conclusion, the investigated $\text{TeO}_3 (0.007\lambda)/3\text{C-SiC} (0.09\lambda)/128^\circ\text{Y-X LiNbO}_3$ multi-layered configuration demonstrates significant potential as an efficient and low-power acoustic-optic device. The obtained acousto-optic figure of merit ($M = 8.56 \times 10^{-12} \text{ s}^3 \text{ kg}^{-1}$) and high diffraction efficiency (96.1%) highlight its favourable performance.

Comparatively, when compared to earlier established materials and layered structures commonly used in acousto-optic devices, the $\text{TeO}_3 (0.007\lambda)/3\text{C-SiC} (0.09\lambda)/128^\circ\text{Y-X LiNbO}_3$ configuration showcases competitive advantages. It offers temperature stability and enables precise control of the acousto-optic interaction. In contrast to single crystal-based acoustic devices, the multi-layered configuration allows for tunability of key properties such as acoustic velocity, electromechanical coupling coefficient, and temperature coefficient of delay.

Furthermore, the $\text{TeO}_3 (0.007\lambda)/3\text{C-SiC} (0.09\lambda)/128^\circ\text{Y-X LiNbO}_3$ configuration outperforms certain well-known materials in terms of its acousto-optic figure of merit and diffraction efficiency. These results emphasize its potential for advanced acousto-optic applications, offering improved performance and energy efficiency.

Overall, the $\text{TeO}_3 (0.007\lambda)/3\text{C-SiC} (0.09\lambda)/128^\circ\text{Y-X LiNbO}_3$ multi-layered configuration exhibits promising features that position it as a compelling choice

for the development of next-generation acousto-optic devices, surpassing some conventional materials and layered structures in terms of performance and tunability. It not only exhibits excellent acousto-optic performance but also offers the advantage of requiring low driving power. Its suitability for various applications in fields such as telecommunications, imaging, sensing, and optical signal processing makes it an attractive option for further exploration and utilization in practical scenarios.

Funding

This research did not receive any specific grant from funding agencies in the public, commercial, or not-for-profit sectors.

Data availability

No data were generated or analyzed in the presented research.

Conflict of interest

The authors declare no conflicts of interest.

References

- [1] Heenkenda R, Hirakawa K, Sarangan A. Tunable optical filter using phase change materials for smart IR night vision applications. *Opt Express* 2021;29:33795–803. <https://doi.org/10.1364/OE.440299>.
- [2] Liu J, Khan ZU, wang C, Zhang H, Sarjoghian S. Review of Graphene modulators from the low to the high figure of merits. *J Phys D Appl Phys* 2020;53:233002. <https://doi.org/10.1088/1361-6463/ab7cf6>.
- [3] Al-Hayali SKM, Al-Janabi AH. Triple-wavelength passively Q-switched ytterbium-doped fibre laser using zinc oxide nanoparticles film as a saturable absorber. *J Mod Opt* 2018;65(13):1559–64. <https://doi.org/10.1080/09500340.2018.1455922>.
- [4] Machikhin AS, et al. Acousto-Optical Deflector For Non-Mechanical Manipulating Using Optical Tweezer. *J Phys: Conf Ser* 2020;1461:012087. <https://doi.org/10.1088/1742-6596/1461/1/012087>.
- [5] Kakio S. Acousto-Optic Modulator Driven by Surface Acoustic Waves. *Acta Phys Pol, A* 2015;127(1):15–9. <https://doi.org/10.12693/APhysPolA.127.15>.
- [6] Duocastella M, surdo S, Zunino A, Diaspro A, Saggau P. Acousto-optic systems for advanced microscopy. *J Phys Photon* 2021;vol. 3:012004. <https://doi.org/10.1088/2515-7647/abc23c>.
- [7] Savage N. Acousto-optic devices. *Nat Photonics* 2010;4:728–9. <https://doi.org/10.1038/nphoton.2010.229>.
- [8] Kapfinger S, Reichert T, Lichtmannecker S, et al. Dynamic acousto-optic control of a strongly coupled photonic molecule. *Nat Commun* 2015;6:8540. <https://doi.org/10.1038/ncomms9540>.
- [9] Tanabe T, Notomi M, Kuramochi E, et al. Trapping and delaying photons for one nanosecond in an ultrasmall high-Q photonic-crystal nanocavity. *Nat Photonics* 2007;1:49–52. <https://doi.org/10.1038/nphoton.2006.51>.
- [10] Smith MJA, Martijn de Sterke C, Wolff C, Lapine M, Poulton CG. Enhanced acousto-optic properties in layered media Vol. 96. *Phys Rev* 2017;064114.
- [11] Belovickis J, Rimeika R, Ciplys D. Acousto-optic interaction with leaky surface acoustic waves in Y-cut LiTaO₃ crystals. *Ultrasonics* 2012;52(5):593–7. <https://doi.org/10.1016/j.ultras.2011.12.004>.
- [12] Colston G, Myronov M. Controlling the optical properties of monocrystalline 3C-SiC heteroepitaxially grown on silicon at low temperatures. *Semicond Sci Technol* 2017;32(1–6):14005. <https://doi.org/10.1088/1361-6641/aa8b2a>.
- [13] Caliendo C, Laidoudi F. Experimental and Theoretical Study of Multi frequency Surface Acoustic Wave Devices in a Single Si/SiO₂/ZnO Piezoelectric Structure. *Sensors* 2020;20:1380. <https://doi.org/10.3390/s20051380>. No. 5.
- [14] Dewan N, Sreenivas K, Gupta V. Temperature-Compensated Devices Using Thin TeO₂ Layer With Negative TCD. In: *IEEE Elec. Dev. Lett.*; 2006. p. 752–4. <https://doi.org/10.1109/LED.2006.880644>. vol. 27 no. 9.
- [15] Soni ND, Bhola J. Enhanced Properties of SAW Device Based on Beryllium Oxide Thin Films. *Crystals* 2021;11(4):332. <https://doi.org/10.3390/cryst11040332>.
- [16] Guofang F, Jiping N, Jisheng Y. The design of ZnO/LiNbO₃ thin-plating surface acoustical waveguide in acousto-optic tunable filters. *Opt Laser Technol* 2007;39(2):421–3. <https://doi.org/10.1016/j.optlastec.2005.06.031>.
- [17] Shandilya S, Sreenivas K, Gupta V. Acousto optic and SAW propagation characteristics of a temperature stable multi-layered structures based on LiNbO₃ and diamond. *J Phys D Appl Phys* 2008;41:1–6. <https://doi.org/10.1088/0022-3727/41/2/025108>.
- [18] Dewan N, Sreenivas K, Gupta V. Theoretical studies on a TeO₂/ZnO/diamond layered structure for zero TCD SAW devices. *Semicond Sci Technol* 2008;23:085002. <https://doi.org/10.1088/0268-1242/23/8/085002>.
- [19] Wang L, et al. Enhanced Performance of 17.7 Ghz Saw Devices Based on AlN/diamond/si Layered Structure With Embedded Nano transducer. *Appl Phys* 2017;111(25):253502. <https://doi.org/10.1063/1.5006884>.
- [20] Zhang H, Wang H. Investigation of Surface Acoustic Wave Propagation Characteristics in New Multilayer Structure: SiO₂/IDT/LiNbO₃/Diamond/Si. *Micromachines* 2021;12(11):1286. <https://doi.org/10.3390/mi12111286>.
- [21] Sharma M, Kaur P, Kumar P. Recent Advances in Acousto-Optic Devices: Materials, Fabrication Techniques, and Applications. In: *Handbook of optoelectronic device modeling and simulation*. Cham: Springer; 2020. p. 341–70.
- [22] Song J, Hu C, Yan Y, Yang Q. Advanced film preparation techniques for acousto-optic devices. In: *Proceedings of the 2016 international conference on advanced mechatronic systems (ICAMEchS)*. IEEE; 2016. p. 223–7.
- [23] Bhaktha SN, Drabe CG. Silicon carbide as a novel material for next-generation acousto-optic devices. *Appl Opt* 2018;57(13):3583–90.
- [24] Chaudhuri S, Kundu M. Zinc oxide-based acousto-optic devices: A review. *J Mater Sci Mater Electron* 2020;31(15):12530–51.
- [25] Parchur AK, Dhoble SJ. Acousto-optic properties of zinc sulfide. *J Appl Phys* 2008;103(11):113506.
- [26] Zhang X, et al. Recent advances in perovskite-based acousto-optic devices. *Adv Opt Mater* 2020;8(20):2000037.
- [27] Soni ND. SAW propagation characteristics of TeO₃/3C-SiC/LiNbO₃ layered structure. *Mat Res Exp* 2018;5:046309. <https://doi.org/10.1088/2053-1591/aabe6b>.
- [28] Fu S, et al. High-Frequency Surface Acoustic Wave Devices Based on ZnO/SiC Layered Structure. *IEEE Electron Device Lett* 2019;40(1):103–6. <https://doi.org/10.1109/LED.2018.2881467>.
- [29] Xu H, et al. Enhanced Coupling Coefficient in Dual-Mode ZnO/SiC Surface Acoustic Wave Devices with Partially Etched Piezoelectric Layer. *Appl Sci* 2021;11(4):6383. <https://doi.org/10.3390/app11146383>.

- [30] Mehregany M, Zorman CA, Roy S, Fleischman AJ, Wu CH, Rajan N. Silicon carbide for microelectromechanical systems. *Int Mater Rev* 2013;45:85–108. <https://doi.org/10.1179/095066000101528322>.
- [31] Garrisi F, Chatzopoulos I, Cernansky R, Politi A. Silicon carbide photonic platform based on suspended sub-wave-length waveguides. *J Opt Soc Am* 2020;B37:3453–60. <https://doi.org/10.1364/JOSAB.403170S>.
- [32] Yamada BS, Song, Asano T, Noda S. Silicon carbide based photonic crystal nano cavities for ultra-broadband operation from infrared to visible wavelengths. *Appl Phys Lett* 2011; 99(20):201102. <https://doi.org/10.1063/1.3647979>.
- [33] Liu YM, Prucnal PR. Low-loss silicon carbide optical waveguides for silicon-based optoelectronic devices. In: *IEEE Phot. Tech. Lett.*; 1993. p. 704–7. <https://doi.org/10.1109/68.219717>. vol. 5 No. 6.
- [34] Soni R, Sharma M, Kumar P. Silicon carbide (SiC) based layered structures for acousto-optic wave devices: A review. *Opt Mater* 2018;84:598–611.
- [35] Fahmy AH, Adler EL. Multilayer acoustic-surface-wave program. In: *Proc IEEE*; 1975. p. 470–2. <https://doi.org/10.1049/piee.1975.0128>. Vol. 122 no. 5.
- [36] Djemia P, Roussigné Y, Dirras G, Jackson K. Elastic properties of β -SiC films by Brillouin light scattering. *J Appl Phys* 2004;95:2324. <https://doi.org/10.1063/1.1642281>.
- [37] Kovacs G, Anhorn M, Engan HE, Visintini G, Ruppel CCW. Improved material constants for LiNbO₃ and LiTaO₃. In: *IEEE symp. Ultras.*; 1990. p. 435–8. <https://doi.org/10.1109/ULTSYM.1990.171403>. vol. 1.
- [38] Cimalla V, Pezoldt J, Ambacher O. Group III Nitride And SiC Based MEMs And NEMs: Materials Properties, Technology And Applications. *J Phys D Appl Phys* 2007;40:6386. <https://doi.org/10.1088/0022-3727/40/20/S19>.
- [39] Djemia P, Bouamama K. Ab-initio calculations of the photoelastic constants of the cubic SiC polytype. *J Phys: Conf Ser* 2013; 454:12060. <https://doi.org/10.1088/1742-6596/454/1/012060>.
- [40] Jain S, Mansingh A. Thin film layered structure for acousto-optic devices. *J Phys D Appl Phys* 1992;25:1116. <https://doi.org/10.1088/0022-3727/25/7/014>.
- [41] Andrushchak S, et al. Complete sets of elastic constants and photoelastic coefficients of pure and MgO-doped lithium niobate crystals at room temperature. *J Appl Phys* 1990;vol. 106:073510. <https://doi.org/10.1063/1.3238507>.
- [42] Rana L, Gupta V, Dewan N, Tomar M. SAW field and Acousto-optical Interaction in ZnO/AlN/Sapphire Structure. In: *Joint IEEE Int Symp Appl Ferro Sep*; 2016. <https://doi.org/10.1109/ISAF.2016.7578095>.
- [43] Mys O, Krupych O, Kostyrko M, Vlokh R. Anisotropy of acousto-optic figure of merit for LiNbO₃ crystals—anisotropic diffraction: erratum. *Appl Opt* 2016;55: 9823–9. <https://doi.org/10.1364/AO.55.009823>.
- [44] Mys O, Kostyrko M, Zapeka B, Krupych O, Vlokh R. Anisotropy of acoustooptic figure of merit for TeO₂ crystals. 2. Anisotr Diffr: Errata 2016;17(4):148. <https://doi.org/10.3116/16091833/17/4/148/2016>. Ukr. J. Phys. Opt.
- [45] Voloshinov VB, Khorkin VS, Kulakova LA, Gupta N. Optic, Acoustic And Acousto-Optic Properties Of Tellurium In Close-To-Axis Regime Of Diffraction. *J Phys Commun* 2017; 1:025006. <https://doi.org/10.1088/2399-6528/Aa86ba>.
- [46] Shih WC, Wang TL, Hsu LL. Surface acoustic wave properties of Aluminum Oxide films on Lithium Niobate. *Thin Solid Films* 2010;518:7143–6. <https://doi.org/10.1016/j.tsf.2010.07.029>.